Enhancing the Frequency Adaptability of Periodic Current Controllers for Grid-Connected Power Converters

Yang, Yongheng; Zhou, Keliang; Blaabjerg, Frede

Published in:
Proceedings of the 2015 IEEE Energy Conversion Congress and Exposition (ECCE)

DOI (link to publication from Publisher):
10.1109/ECCE.2015.7310501

Publication date:
2015

Document Version
Early version, also known as pre-print

Enhancing the Frequency Adaptability of Periodic Current Controllers for Grid-Connected Power Converters

Yongheng Yang[†1], *IEEE Member*, Keliang Zhou[‡2], *IEEE Senior Member*, and Frede Blaabjerg[†3], *IEEE Fellow*

[†]Department of Energy Technology
Aalborg University
Aalborg, DK-9220 Denmark
[1]yoy@et.aau.dk; [3]fbl@et.aau.dk

[‡]School of Engineering
University of Glasgow
Glasgow, G12 8QQ Scotland, United Kingdom
[2]keliang.zhou@glasgow.ac.uk

***Abstract*— It is mandatory for grid-connected power converters to synchronize the feed-in currents with the grid. Moreover, the power converters should produce feed-in currents with low total harmonic distortions according to the demands, by employing advanced current controllers, e.g., Proportional Resonant (PR) and Repetitive Controllers (RC). The synchronization is actually to detect the instantaneous grid information (e.g., frequency and phase of the grid voltage) for the current control, which is commonly performed by a Phase-Locked-Loop (PLL) system. As a consequence, harmonics and deviations in the estimated frequency by the PLL could lead to current tracking performance degradation, especially for the periodic signal controllers (e.g., PR and RC) of high frequency-dependency. In this paper, the impacts of frequency deviations induced by the PLL and/or the grid disturbances on the selected current controllers are investigated by analyzing the frequency adaptability of these current controllers. Subsequently, strategies to enhance the frequency-variation-immunity for the current controllers are proposed for the power converters to produce high quality feed-in currents even in the presence of frequency deviations. Experiments on a single-phase grid-connected inverter system are presented, which have verified the proposals and also the effectiveness of the frequency adaptive current controllers.**

I. Introduction

Power electronics converters have been widely used in grid-connected renewable energy systems like wind turbine systems and PhotoVoltaic (PV) systems [1], [2]. However, due to their non-linearity and also the intermittency, harmonic challenges are also associated with the power electronics interfaced renewable energy systems, which have to be dealt with by employing advanced control strategies according to the demands [3]. Commonly, a two-cascaded control system is adopted in the grid-connected power converters [4]. Since the inner current controller of the cascaded loops is responsible for shaping the current (i.e., power quality issues), great efforts have been devoted to the control of the feed-in grid current, which is also required to be synchronized with the grid voltage. Phase Locked Loop (PLL) systems are widely used in the grid-connected inverters for synchronization [5]–[8]. Hence, the information (especially the grid frequency) provided by a PLL system is of importance for the current controllers, and it is extensively used at different levels of the entire control system (e.g., reference transformation).

The current control can be implemented in the rotating reference frame (dq), the stationary reference frame ($\alpha\beta$), or the three-phase natural reference frame (abc) [4], [9], [10]. Taking the control in the dq-frame for an example, Park and/or Clarke transforms enable the employment of Proportional Integrator (PI) controllers, where the PLL estimated grid frequency is a must for the transforms. Consequently, either frequency variations in the grid or the frequency estimation error by a PLL system will result in control degradations when using PI controllers. On the other hand, in order to simplify the control, periodic signal controllers like Repetitive Controller (RC) [11]–[15] and Proportional Resonant (PR) controller with parallel RESonant (RES) based harmonic compensators [4], [14], [16]–[18] are developed in either the $\alpha\beta$- or the abc-frame. In that case, the control accuracy of both the PR with RES or RC controllers is strongly affected by the designed center frequency of the resonant controller [12], [16]. Basically, the center frequency (e.g., the fundamental frequency – 50 Hz) should be placed at which the control gain can approach infinite, and a constant value is selected for simplicity. Thus, the frequency deviations will result in a finite control gain at the resonant frequencies.

Additionally, an online update of the center frequency is enabled by feeding back the PLL estimated frequency to the current controller in order to enhance the control performance. However, the grid voltage as the input of the PLL systems cannot always be maintained as "constant" in terms of amplitude, frequency, and/or phase, due to multiple eventualities like continuous connection and disconnection of loads and fault to ground because of lightning strikes [19], [20]. That is why the grid codes also demand that the power converters should be able to operate within a specified frequency range or even regulate the frequency [21]. Together with background distortions, a large obstacle has been posed for the PLL systems. As a result, the current controllers in the $\alpha\beta$- or the abc-frame will inevitably suffer from frequency deviations

978-1-4673-7151-3/15/$31.00

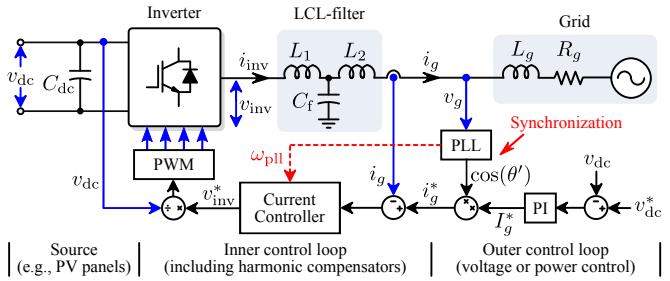

Fig. 1. Overall dual-loop control structure of a single-phase grid-connected system with an LCL filter and a PLL synchronization unit.

either due to the PLL errors or the grid disturbances [11], [12], [22], resulting in a possibility for the feed-in current to reach the Total Harmonic Distortions (THD) limits [3]. Thus, advanced synchronizations (e.g., PLL systems) are desirable in order to ensure a reliable and satisfactory control of the grid current, and also it is essential to enhance the frequency adaptability of the periodic current controllers [13], [23]–[28].

In view of the above issues, in this paper, the frequency adaptability of the selected periodic current controllers (i.e., PR, RES, and RC) is explored in the consideration of the PLL estimated frequency variations owing to either the PLL inherent errors or the grid disturbances. In § II, a brief description of the dual-loop control method for single-phase grid-connected inverters is presented. Then, the frequency adaptability of the periodic current controllers is focused on. More important, solutions to enhance the frequency adaptability of these current controllers are also proposed, being the frequency adaptive current controllers. The discussions and the effectiveness of the frequency adaptive current controllers are verified by experiments in § IV before the conclusion.

II. Frequency Adaptability Analysis

A. Control of Single-Phase Grid-Connected Converters

Fig. 1 shows a typical configuration of a single-phase grid-connected system and its overall cascaded dual-loop control structure, where an LCL-filter is used considering the power quality issues [4]. It is shown in Fig. 1 that the PLL estimated grid frequency (ω_{pll}) is feeding back to the current controller as aforementioned in order to improve the control performance. Especially, the frequency ω_{pll} is used to transform AC quantities (i.e., the grid current i_g and voltage v_g) to DC quantities (i.e., $\mathbf{i}_{\text{dq}}$ and $\mathbf{v}_{\text{dq}}$) for PI controllers in the dq-frame or reversely ($dq \rightarrow \alpha\beta$). Yet for simplicity in the case of the current control in either the $\alpha\beta$- or the abc-frame, a fixed constant frequency (i.e., the nominal grid frequency ω_0) is designed for the periodic current harmonic controllers in practice (especially, when implemented in a digital signal processor), as it is shown in Fig. 2. In both cases, the current controller performance will be affected by the PLL estimated frequency, which is used to generate the grid current reference according to Fig. 1. Notably, other current controllers like the Dead-Beat (DB) control can also be used as the fundamental-frequency current controller [29], [30].

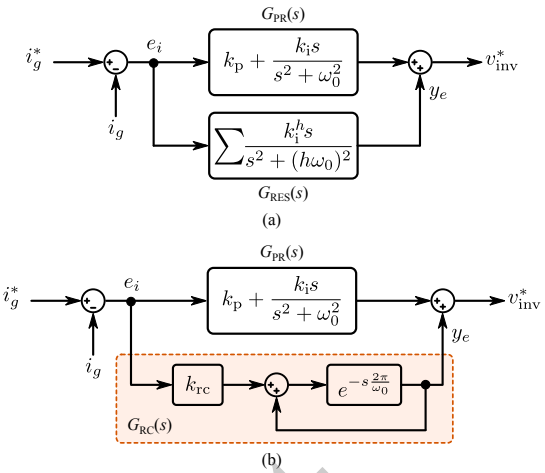

Fig. 2. Proportional resonant current controller $G_{\text{PR}}(s)$ with (a) resonant harmonic controller $G_{\text{RES}}(s)$ and (b) repetitive harmonic compensator $G_{\text{RC}}(s)$.

B. Frequency Sensitivity Analysis of the Current Controllers

In practice, it is difficult to attain an acceptable feed-in current even with high-order grid filters (e.g., an LCL-filter) because of the always existing background distortions in the grid voltage. Thus, harmonic compensators are typically incorporated in the current control loop, as it is shown in Fig. 2, where the fundamental-frequency current controller (i.e., $G_{\text{PR}}(s)$) can be given as

$$G_{\text{PR}}(s) = k_{\text{p}} + \frac{k_{\text{i}} s}{s^2 + \omega_0^2} \tag{1}$$

in which k_{p} and k_{i} are the control gains. It can be seen in Fig. 2 that the harmonic compensator embraces either a paralleled multi-resonant controller $G_{\text{RES}}(s)$ or a repetitive controller $G_{\text{RC}}(s)$, which is effective only in the $\alpha\beta$-frame. Accordingly, the harmonic compensators can be expressed as

$$G_{\text{RES}}(s) = \sum_{h=3,5,7,\cdots} G^h_{\text{RES}}(s) \tag{2}$$

$$G_{\text{RC}}(s) = \frac{k_{\text{rc}} e^{-2\pi s/\omega_0}}{1 - e^{-2\pi s/\omega_0}} \tag{3}$$

where $G^h_{\text{RES}}(s)$ is the h^{th}-order resonant controller with h being the harmonic order and k_{rc} is the control gain of the RC harmonic compensator. Furthermore, the individual resonant controller can be given as

$$G^h_{\text{RES}}(s) = \frac{k^h_{\text{i}} s}{s^2 + (h\omega_0)^2} \tag{4}$$

in which k^h_{i} is the control gain of the corresponding h^{th}-order resonant controller. In addition, the RC based harmonic controller can further be expanded into [30]

$$G_{\text{RC}}(s) = k_{\text{rc}} \left[-\frac{1}{2} + \frac{\omega_0}{2\pi s} + \frac{\omega_0}{\pi} \sum_k \frac{s}{s^2 + (k\omega_0)^2} \right] \tag{5}$$

with k = 1, 2, 3, $\cdots$. Eq. (5) indicates the inherent resonant characteristic of the RC controller with an identical resonant

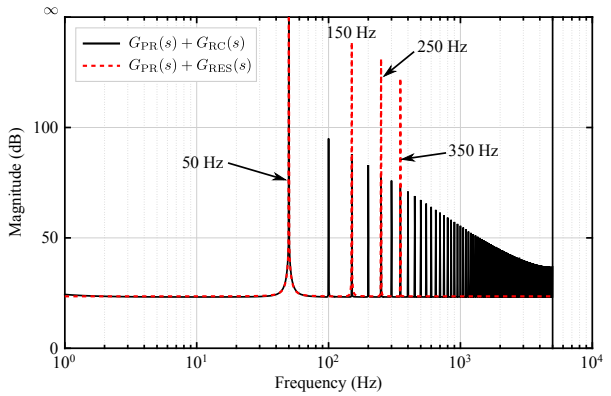

Fig. 3. Magnitude response of the current controllers shown in Fig. 2, where h = 3, 5, 7.

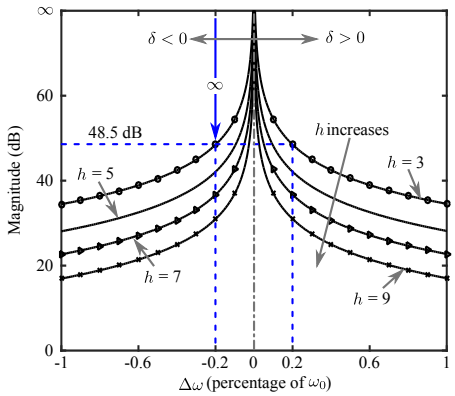

Fig. 4. Magnitudes of the resonant controller $G^h_{\text{RES}}(s)$ as a function of the frequency variation $\Delta\omega$, where k^3_{i} = 1000, k^5_{i} = 800, k^7_{i} = 600, and k^9_{i} = 400.

gain (i.e., $k_{\text{rc}}\omega_0/\pi$), and it also shows that the internal models of the DC signal and all harmonics are incorporated in the harmonic compensator $G_{\text{RC}}(s)$.

According to Fig. 2, the error rejection transfer function $G_e(s)$ can be given as

$$G_e(s) = \frac{E_i(s)}{I_g^*(s)} = \frac{1}{1 + [G_{\text{CC}}(s) + G_{\text{HC}}(s)]\, G_{\text{P}}(s)} \tag{6}$$

with $G_{\text{CC}}(s)$ being the fundamental-frequency current controller (e.g., PR or DB controllers), $G_{\text{HC}}(s)$ being the harmonic compensators (e.g., RES or RC controllers), and $G_{\text{P}}(s)$ being the plant model. When $s \to jk\omega_0$, it can be seen from (1)-(5) that the magnitude response of these controllers will theoretically approach to infinite (i.e., $|G_{\text{CC}}(jk\omega_0) + G_{\text{HC}}(jk\omega_0)| \to \infty$), as illustrated in Fig. 3. Consequently, the tracking error $e_i(t)$ ($E_i(s)$ in (6)) will be zero at the frequencies of interest (i.e., $k\omega_0$). In other words, the RES controller enables a selective harmonic compensation, while the RC controller can eliminate all harmonics below the Nyquist frequency theoretically, being a good alternative for harmonic control [12], [13], [31].

However, in practical applications, the grid frequency is not exactly the nominal one ω_0 but a time-varying element of the grid voltage with small deviations. In that case, infinite magnitudes of those current controllers can not always be maintained when $s \to jk\omega_{\text{pll}}$, leading to reduced tracking performance and thus a poor THD of the feed-in current. Even with an advanced PLL system, the frequency deviations can not be completely eliminated. In general, the PLL estimated frequency ω_{pll} can be expressed as

$$\omega_{\text{pll}} = \omega_0 + \Delta\omega \tag{7}$$

in which $\Delta\omega = \Delta\omega_g + \Delta\omega_{\text{pll}}$ represents the estimated angular frequency deviations. It consists of the grid frequency disturbances $\Delta\omega_g = \omega_g - \omega_0$ with ω_g being the instantaneous grid frequency and/or the PLL tracking errors $\Delta\omega_{\text{pll}}$. As discussed above, (1)-(5) and (7) imply that a small frequency variation (i.e., $\Delta\omega$) induced by the grid frequency changes and/or PLL estimation errors can contribute to a degradation of the error rejection capability for those current controllers, which are supposed to approach to infinite at the targeted frequencies (i.e., $k\omega_{\text{pll}}$). This impact is referred to as the frequency adaptability, which is illustrated as the following.

According to (4) and (7), the magnitude response (i.e., $s = jh\omega_{\text{pll}}$) of an individual resonant controller $G^h_{\text{RES}}(s)$ at the corresponding frequency ($h\omega_{\text{pll}}$) can be obtained as

$$\left|G^h_{\text{RES}}(jh\omega_{\text{pll}})\right| = \left|\frac{jk^h_{\text{i}}h\omega_{\text{pll}}}{-h^2\omega^2_{\text{pll}} + h^2\omega^2_0}\right| = \frac{k^h_{\text{i}}}{h\omega_0}\left|\frac{\delta+1}{\delta^2+2\delta}\right| \tag{8}$$

with $\delta = \Delta\omega/\omega_0$, and Eq. (8) indicates that the gain will not be infinite unless δ = 0 (i.e., $\Delta\omega$ = 0). The control gain reduction of the resonant controllers due to the frequency variations $\Delta\omega$ is illustrated in Fig. 4, where it can be observed that even a small frequency variation of $\pm$0.2% can result in a significant performance degradation of the resonant controllers (e.g., the magnitude decreases from ∞ dB to 48.5 dB). It demonstrates that the RES based harmonic compensator (and also the PR controller with h = 1) is sensitive to frequency variations. In other words, the RES controller in (4) has a poor frequency-variation-immunity.

In the same manner, substituting $s = jh\omega_{\text{pll}}$ into (3) gives the magnitude response of the RC controller G_{RC} as

$$\left|G_{\text{RC}}(jh\omega_{\text{pll}})\right| = \left|\frac{k_{\text{rc}}e^{-j\cdot 2\pi h(1+\delta)}}{1 - e^{-j\cdot 2\pi h(1+\delta)}}\right| \tag{9}$$

According to the Euler's formula, the following is obtained

$$\left|G_{\text{RC}}(jh\omega_{\text{pll}})\right| = \frac{k_{\text{rc}}}{\sqrt{2 - 2\cos(2\pi h\delta)}} \tag{10}$$

which implies that the RC controller no longer can approach infinite control gain when there is a frequency tracking error from the PLL system (and/or grid frequency changes), i.e., $\delta \neq 0$ and $\Delta\omega \neq 0$. Fig. 5 further illustrates the effect of a frequency deviation on the current control error rejection ability of the RC harmonic compensator. As it can be observed in Fig. 5, a remarkable gain drop (e.g., the magnitude decreases from ∞ dB to 28.5 dB) occurs due to a frequency change of

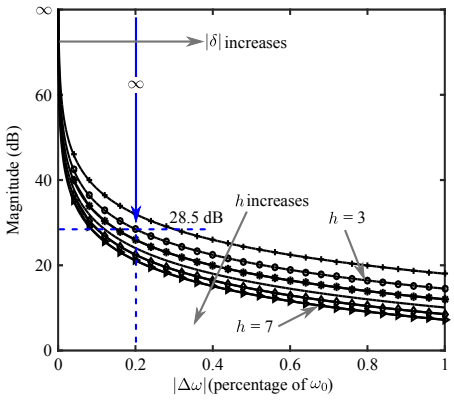

Fig. 5. Magnitudes of the repetitive controller $G_{\mathrm{RC}}(s)$ as a function of the frequency variation $\Delta\omega$, where k_{rc} = 1.

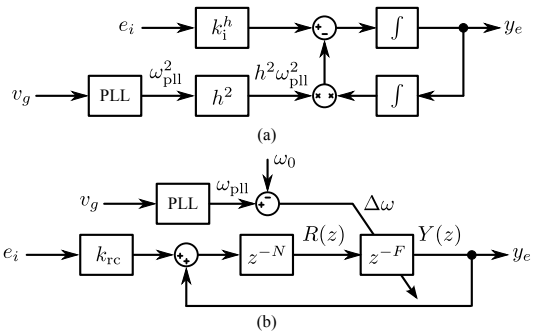

Fig. 6. Frequency-variation-immunity enhanced periodic current harmonic compensators: (a) resonant controllers and (b) repetitive controller.

TABLE I
COEFFICIENTS OF THE LAGRANGE INTERPOLATING POLYNOMIAL BASED FRACTIONAL DELAY FILTER z^{-F} (F: THE FILTER ORDER).

H_l	$L = 1$ (Linear)	$L = 3$ (Cubic)
H_0	$1 - F$	$-(F-1)(F-2)(F-3)/6$
H_1	F	$F(F-2)(F-3)/2$
H_2		$-F(F-1)(F-3)/2$
H_3		$F(F-1)(F-2)/6$

± 0.2 % (i.e., corresponding to a frequency variation of ± 0.1 Hz in 50-Hz systems), and consequently the rejection ability is significantly degraded. A conclusion drawn from Figs. 4 and 5 is that the frequency sensitivity of the periodic current controllers (i.e., the PR, RES, and RC controllers) is poor, and thus enhancing the frequency adaptability is necessary in order to produce high-quality currents.

III. Enhancing the Frequency Adaptability

As discussed in the last paragraph, in order to achieve a good current control in terms of a zero-error elimination of the harmonics even under a variable grid frequency (or a PLL tracking error), the current controllers have to be frequency adaptive. It means that the control gain should be infinite when $s = jh\omega_{\mathrm{pll}}$. Thus, feeding back the frequency estimated by an advanced PLL system to the current controllers is a possibility to decrease the frequency sensitivity. This is much convenient for the resonant controllers [23]–[25], which is given as

$$G^{h}_{\mathrm{RES}}(s) = \frac{k^{h}_{\mathrm{i}} s}{s^2 + (h\omega_{\mathrm{pll}})^2} = \frac{k^{h}_{\mathrm{i}} s}{s^2 + [h(\omega_0 + \Delta\omega)]^2} \tag{11}$$

Fig. 6(a) shows the implementation of a frequency adaptive resonant controller. It can be observed in Fig. 6(a) and (11) that, by feeding in the PLL estimated frequency, the resonant frequencies of the harmonic controllers $G^{h}_{\mathrm{RES}}(s)$ will automatically be adjusted to the instantaneous grid frequency. As a result, infinite gains of the resonant controllers are attained in the case of a varying grid frequency.

However, in respect to the RC controller, enhancing the frequency adaptability cannot be reached by simply feeding back the PLL estimated frequency, since the RC controller is normally implemented in a digital signal processor of a fixed sampling rate. In that case, the RC controller shown in (3) can be given as

$$G_{\mathrm{RC}}(z) = \frac{k_{\mathrm{rc}} z^{-(N+F)}}{1 - z^{-(N+F)}} \tag{12}$$

in which $N = \lfloor f_s/f \rfloor$ is an integer, $F = f_s/f - N$ is the order of a fractional delay (i.e., z^{-F}) with $f = \omega_{\mathrm{pll}}/(2\pi)$, and f_s is the sampling frequency. Therefore, to enhance the frequency adaptability of the RC controller, one possibility is that the fractional delay z^{-F} induced by the frequency variations should be appropriately approximated. A cost-effective approach to approximate the fractional delay is using Finite-Impulse-Response (FIR) filters as discussed in [12], [32]. It should be noted that, the frequency adaptability of the RC harmonic compensator can be enhanced alternatively by varying the sampling frequency [13], which should ensure an integer of f_s/f (i.e., $F = 0$) in practical applications, but it will increase the cost and the overall complexity.

The most popular but simple and effective solution to the FIR fractional delay z^{-F} is based on the Lagrange interpolating polynomial, which can be expressed as

$$z^{-F} \approx \sum_{l=0}^{L} \left(z^{-l} H_l\right) = \sum_{l=0}^{L} \left(z^{-l} \prod_{\substack{i=0 \\ i \neq l}}^{L} \frac{F-i}{l-i} \right) \tag{13}$$

where H_l is the Lagrange interpolating polynomial coefficient, $l, i = 0, 1, 2, \ldots, L$, and L is the length of the Lagrange interpolation based fractional delay filter. For convenience, the coefficients of the Lagrange based fractional delay filter z^{-F} are given in Table I. If L = 1, Eq. (13) corresponds to a linear interpolation between two samples, i.e., $z^{-F} \approx H_0 + H_1 z^{-1}$. While in the case of L = 3, a cubic interpolating polynomial is formulated, i.e., $z^{-F} \approx H_0 + H_1 z^{-1} + H_2 z^{-2} + H_3 z^{-3}$, which has been proved in [12], [30], [32] as a relatively good and accurate approximation of the fractional delay z^{-F} in terms of the bandwidth and also the resultant phase delay. Thus, it can be employed to enhance the frequency-variation-immunity of the RC controller. Following, the general block diagram of a frequency adaptive RC harmonic compensator can be constructed as shown in Fig. 6(b).

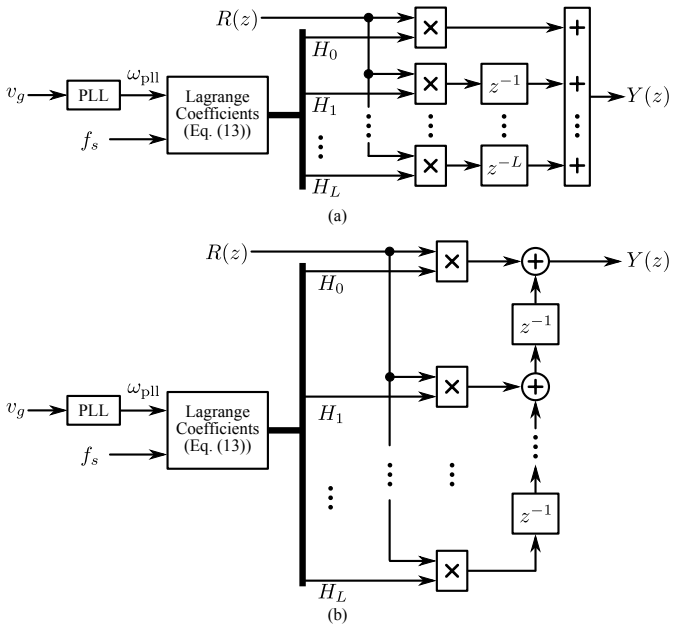

Fig. 7. Different implementations of the fractional delay filter, where $z^{-F} = Y(z)/R(z)$: (a) a parallel structure [12] and (b) the Farrow structure [32].

TABLE II

COMPLEXITY COMPARISON OF THE FRACTIONAL DELAY FILTER IMPLEMENTATIONS (FIG. 7).

	Parallel structure	Farrow structure
No. of summations	L	L
No. of multiplications	$L+1$	$L+1$
No. of delays	$L(L+1)/2$	L
Structure type	In-parallel	Series connection

TABLE III

PARAMETERS OF THE SINGLE-PHASE SYSTEM SHOWN IN FIG. 1.

Parameter	Symbol	Value
Nominal grid voltage amplitude	v_{gn}	311 V
Nominal grid frequency	ω_0	$2\pi\times50$ rad/s
Rated power	P_{n}	1 kW
Reference current amplitude	I_g^*	5 A
DC-link voltage	v_{dc}	400 V
DC-link capacitor	C_{dc}	1100 μF
Grid impedance	L_g	2 mH
	R_g	0.2 Ω
LCL filter	L_1, L_2	3.6 mH
	C_{f}	2.35 μF
Switching and sampling frequencies	f_{sw}, f_{s}	10 kHz

Although the Lagrange-interpolation-polynomial based fraction delay filter has several advantages like easy formulas for the coefficients and good response at the low frequencies [32], it may still consume certain memory space if not efficiently implemented in the digital control systems. Moreover, when comparing the frequency adaptive schemes for the RES and RC controllers in Fig. 6, the frequency delay order F has an indirect mapping relationship with the frequency variations $\Delta\omega$, requiring an online calculation of the Lagrange coefficients according to the PLL estimated angular frequency ω_{pll} and the system sampling frequency f_s.

Fig. 7 gives two possibilities to implement digitally the fractional delay filter of (13) in low-cost digital signal processors. It can be observed that the Farrow structure [32] has less delay units and thus consumes less memory space compared to the direct structure that has been employed in [12]. Thus, the Farrow structure is a more efficient implementation of the fractional delay filter. Table II further summaries the computational burden (complexity) of the two fractional delay filter structures. It can be seen that, in terms of implementation, the frequency adaptive scheme for the RC harmonic compensator is more complicated than that for the RES controller. Nevertheless, the above discussions have revealed that an advanced PLL system in terms of accuracy and dynamics is crucial for the enhancement of the controller frequency adaptability, especially for single-phase grid-interfaced converters.

IV. EXPERIMENTAL VERIFICATIONS

A. Test-Rig Description

In order to verify the above analysis and also to test the effectiveness of the enhanced frequency adaptability of the current controllers, experiments have been carried out on a single-phase grid-connected inverter system referring to Fig. 1, where an AC programmable power source has been used in order to change the frequency. The system parameters are listed in Table III. For comparison, a DB controller and the PR controller are adopted as the fundamental-frequency current controller, and the RES and RC controllers are used to compensate the harmonics. As for the synchronization, a second order generalized integrator based PLL algorithm [4], [5] has been adopted due to its robust immunity to background distortions and fast dynamics. In the experiments, a commercial DC power supply has been used, and thus the current amplitude reference has been set directly as shown in Table III.

B. Discrete Current Controllers

Since the control systems were done in a dSPACE DS 1103 system, the resonant controller can easily be implemented in a discrete form using one Forward Euler method and one Backward Euler method [5], [24]. Then, the frequency adaptive RES harmonic compensator can be obtained in its discrete form as

$$G_{\text{RES}}^{h}(z) = \frac{(z^{-1}-z^{-2})T_s}{1+(h^2\omega_{\text{pll}}^2T_s^2-2)z^{-1}+z^{-2}} \tag{14}$$

with $T_s = 1/f_s$ being the sampling period. Notably, other discretization methods like the Tustin with pre-warping, the impulse invariant, and the Trapezoidal method can be employed to discretize the resonant controller of (4) at the cost of increased complexity [5]. While for the DB controller, it can be expressed as

$$G_{\text{DB}}(z) = \frac{z^{-1}}{(1-z^{-1})G_f(z)} \tag{15}$$

TABLE IV

PARAMETERS OF THE CURRENT CONTROLLERS/COMPENSATORS.

Controller	Symbol	Value
PR controller	$k_{\rm p}$, $k_{\rm i}$	22, 2000
Resonant controller (RES)	$k_{\rm i}^3$, $k_{\rm i}^5$, $k_{\rm i}^7$	1000
Repetitive controller (RC)	$k_{\rm rc}$	1.8
Low pass filter $Q(z)$	α_0, α_1	0.8, 0.1
Phase-lead compensator $C(z)$	m	3

where $G_f(z)$ is the filter model. In practice, a low pass filter is incorporated into the RC controller in order to improve the controller robustness [30]. Then, the RC harmonic compensator of (3) is modified as given by

$$G_{\rm RC}(z) = \frac{k_{\rm rc} z^{-(N+F)} Q(z)}{1 - z^{-(N+F)} Q(z)} \cdot C(z) \qquad (16)$$

in which $Q(z) = \alpha_1 z + \alpha_0 + \alpha_1 z^{-1}$ is the low pass filter with $\alpha_0 + 2\alpha_1 = 1$ and α_0, $\alpha_1 > 0$, and $C(z) = c^m$ is a phase-lead compensator. The phase-lead number m is determined by experiments. All the parameters of these controllers are shown in Table IV, where it can be seen that only the 3rd, 5th, and 7th RES controllers were incorporated with the fundamental-frequency controller (i.e., the PR controller).

C. Experimental Results

The frequency adaptability of the discussed current controllers in the case of a varying grid frequency has firstly been tested, and the results are shown in Fig. 8, where the grid frequency was programmed within a range of 49.5 Hz to 50.5 Hz (i.e., ± 1 %). It can be observed in Fig. 8 that the DB controller is immune to frequency deviations due to its model-dependent characteristic, while the PR controller is significantly affected by the frequency changes. Specifically, when the grid frequency increases, the performance of the PR controller is significantly degraded, thus resulting in a poor current THD that may exceed the limitation (e.g., THD < 5%) [3]. In addition, it is also shown in Fig. 8 that both the RES and the RC periodic signal controllers present poor frequency adaptability, since they are highly frequency-dependent controllers. The test results are in a close agreement with the analysis presented in § II.B (Fig. 4).

Moreover, the poor frequency adaptability is further verified by the steady-state performance of the RES and RC controllers under a severe abnormal grid frequency (i.e., $2\pi \times 49$ rad/s), as it is shown in Fig. 9. It is observed in Fig. 9 that there will be a phase shift between the grid voltage v_g and the feed-in grid current i_g due to the frequency deviation, and thus leading to a poor power factor. That is to say, the grid-connected inverter system is not operating at unity power factor mode, which may violate the integration demands. Those experimental results have demonstrated the frequency-variation-immunity of the selected current controllers.

According to the discussions in § III, the strategies to enhance the frequency adaptability of the periodic current controllers were applied and the single-phase grid-connected inverter system has been tested. Fig. 10 shows the steady-state

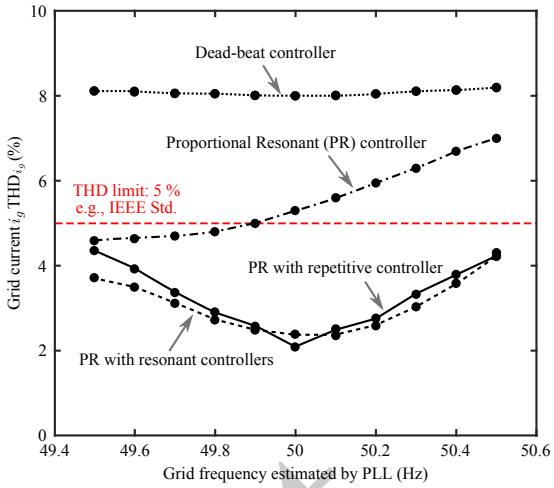

Fig. 8. Experimental verification of the frequency adaptability of the dead-beat and proportional resonant fundamental-frequency current controllers, and the resonant and repetitive based harmonic controllers.

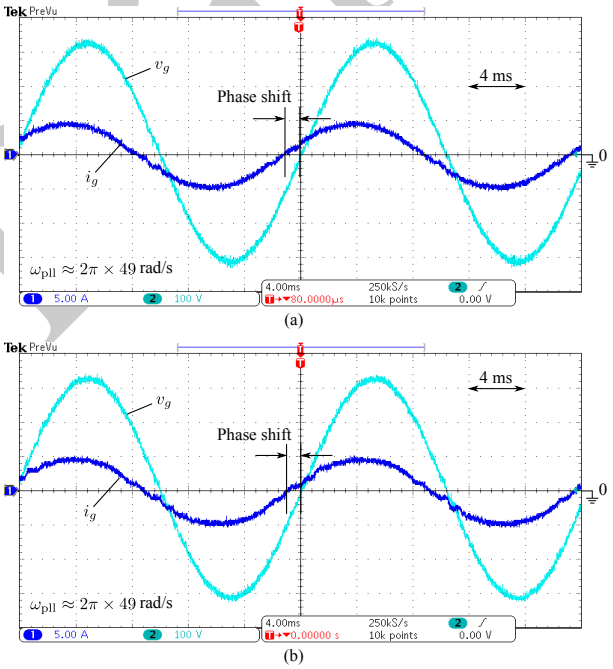

Fig. 9. Steady-state performance of the proportional resonant controller with harmonic compensators (CH1 - grid current i_g [5 A/div]; CH2 - grid voltage v_g [100 V/div]): (a) resonant controllers and (b) the repetitive controller, where the grid frequency is 49 Hz.

performances of the enhanced current controllers. It can be observed in Fig. 10 that, when the PLL estimated frequency $\omega_{\rm pll}$ is fed back to the resonant controller of (14), the tracking performance is improved. As a result, in the case of frequency variations induced by PLL tracking errors and/or the grid disturbances, a unity power factor operation as well as an improved current quality is always achieved. Similarly, when applying the frequency adaptive scheme to the RC harmonic compensator, there is no phase shift between the grid voltage and the injected grid current as shown in Fig. 10(b), and

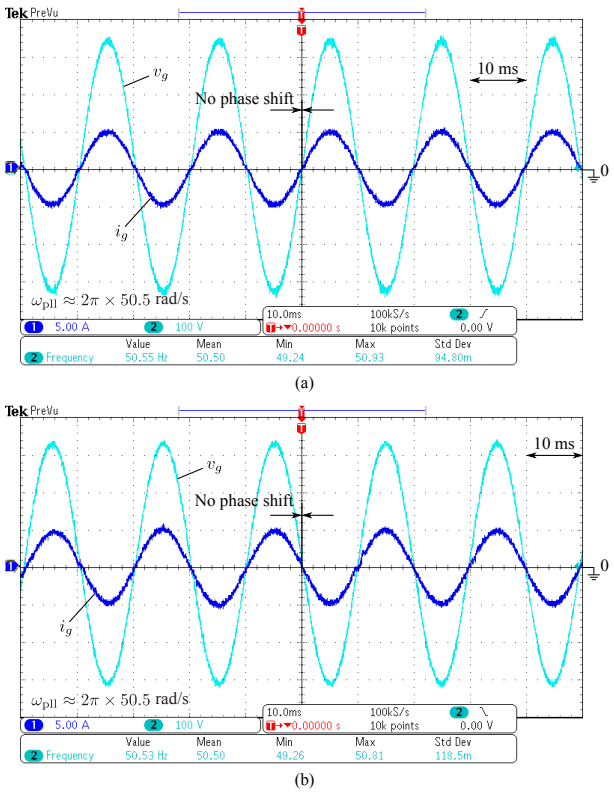

Fig. 10. Steady-state performance of the frequency adaptive current controllers (CH1 - grid current i_g [5 A/div]; CH2 - grid voltage v_g [100 V/div]): (a) resonant controllers and (b) the repetitive controller, where the grid frequency is 50.5 Hz and a frequency adaptive PR controller is employed as the fundamental-frequency current controller.

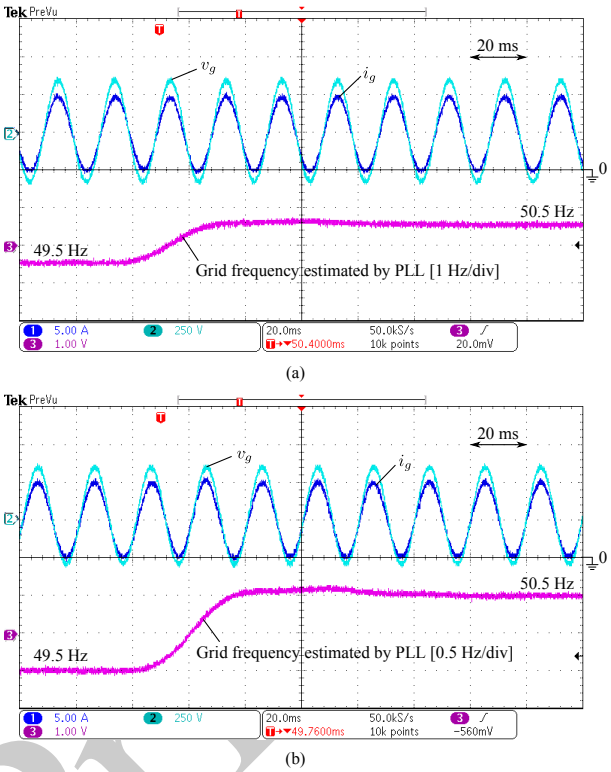

Fig. 11. Dynamic performance of the frequency adaptive proportional resonant with harmonic compensators (CH1 - grid current i_g [5 A/div]; CH2 - grid voltage v_g [100 V/div]; CH3 - PLL output frequency): (a) frequency adaptive resonant controllers and (b) the frequency adaptive repetitive compensator, where the grid frequency changed from 49.5 Hz to 50.5 Hz.

i.e., the system is operating at a unity power factor to feed in high-quality currents. It should be pointed out that the parallel structure shown in Fig. 7(a) is adopted for adapting the RC harmonic controller to grid frequency changes without considering the implementation efficiency.

In addition, the dynamics of the frequency adaptive schemes were tested in the case of a grid-frequency step change (i.e., from 49.5 Hz to 50.5 Hz). The experimental results are presented in Fig. 11, which has verified the effectiveness of the proposed frequency adaptive schemes in terms of dynamics. Similar conclusions can be drawn: it is convenient to feed back the PLL estimated frequency according to Fig. 6(a) in such a way that the frequency adaptability of the RES controller is effectively improved; while by approximating the fractional order delay according to Fig. 7(a), the frequency adaptability of the RC harmonic controller is also enhanced. Both will contribute to an improved power factor as well as a lower THD of the feed-in currents.

Fig. 12 has further validated the effectiveness of the proposed schemes to enhance the frequency-variation-immunity of the current controllers under a wide range of grid frequency variations. When compared with the THD_{i_g} shown in Fig. 8, it can be observed in Fig. 12 that the periodic current controllers with the proposed frequency adaptability schemes can maintain an almost constant THD despite the variations

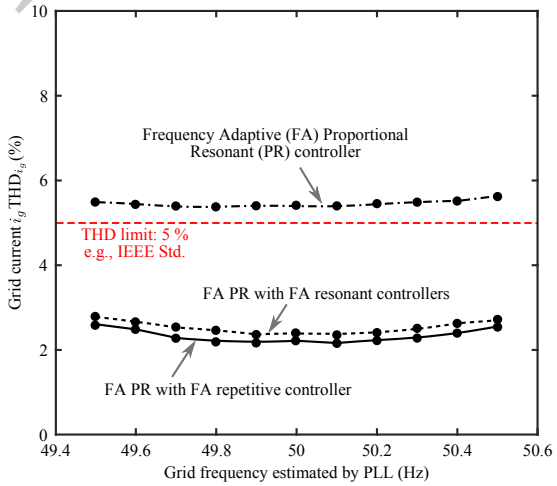

Fig. 12. Performance (experimental verification) of the proportional resonant controller with and w/o harmonic compensators (i.e., resonant controllers or the repetitive controller), where the frequency-variation-immunity is enhanced according to Fig. 6 and Fig. 7.

of the grid frequency (or the PLL estimated frequency). It is also worth to point out that the RC harmonic controller consists of all the resonant controllers with the corresponding frequency below the Nyquist frequency. As a consequence, for the PR controller with a repetitive controller as the harmonic

compensator, the grid current THD is lower than that in the case when the resonant controllers are paralleled as the harmonic compensator, where only a number of harmonics are compensated.

V. Conclusion

The sensitivity to frequency variations of selected current controllers for grid-connected power converters has been explored in this paper. The investigation has revealed that the dead-beat current controller is immune to frequency deviations since it is a model-based predictive controller. In contrast, the resonant (RES) controller and the repetitive controllers (RC) are very sensitive to the frequency variations induced by the PLL control errors and/or the grid disturbances. This is because both periodic current controllers are strongly dependent on the center frequencies, and infinite control gains at the frequencies of interest (e.g., the fundamental frequency) cannot be achieved due to the frequency deviations. In addition, this paper has also introduced means to enhance the frequency adaptability of the discussed current controllers – simply feeding back the PLL estimated frequency to the RES controller or properly approximating the fractional delay for the RC harmonic controller. Experiments performed on a single-phase grid-connected inverter have verified the discussions.

References

[1] J.D. van Wyk. and F.C. Lee, "On a future for power electronics," *IEEE J. Emerg. Sel. Top. Power Electron.*, vol. 1, no. 2, pp. 59–72, Jun. 2013.

[2] F. Blaabjerg, K. Ma, and Y. Yang, "Power electronics - the key technology for renewable energy systems," in *Proc. of EVER*, pp. 1-11, Mar. 2014.

[3] "IEEE recommended practice for utility interface of photovoltaic (PV) systems," *IEEE Std 929-2000*, 2000.

[4] F. Blaabjerg, R. Teodorescu, M. Liserre, and A.V. Timbus, "Overview of control and grid synchronization for distributed power generation systems," *IEEE Trans. Ind. Electron.*, vol. 53, no. 5, pp. 1398–1409, Oct. 2006.

[5] M. Ciobotaru, R. Teodorescu, and F. Blaabjerg, "A new single-phase PLL structure based on second order generalized integrator," in *Proc. of PESC*, pp. 1-6, Jun. 2006.

[6] S.A. Khajehoddin, M. Karimi-Ghartemani, A. Bakhshai, and P. Jain, "A power control method with simple structure and fast dynamic response for single-phase grid-connected DG systems," *IEEE Trans. Power Electron.*, vol. 28, no. 1, pp. 221–233, Jan. 2013.

[7] R.M. Santos Filho, P.F. Seixas, P.C. Cortizo, L.A.B. Torres, and A.F. Souza, "Comparison of three single-phase PLL algorithms for UPS applications," *IEEE Trans. Ind. Electron.*, vol. 55, no. 8, pp. 2923–2932, Aug. 2008.

[8] S. Golestan, M. Monfared, F.D. Freijedo, and J.M. Guerrero, "Design and tuning of a modified power-based PLL for single-phase grid-connected power conditioning systems," *IEEE Trans. Power Electron.*, vol. 27, no. 8, pp. 3639–3650, Aug. 2012.

[9] Y. Yang and F. Blaabjerg, "Overview of single-phase grid-connected photovoltaic systems," *Electric Power Component Sys.*, vol. 43, no. 12, pp. 1352–1363, 2015.

[10] R. Teodorescu, M. Liserre, and P. Rodriguez, *Grid converters for photovoltaic and wind power systems*. Piscataway, NJ, USA: IEEE Press / John Wiley & Sons, 2011.

[11] Y. Song and H. Nian, "Sinusoidal output current implementation of DFIG using repetitive control under generalized harmonic power grid with frequency deviation," *IEEE Trans. Power Electron.*, vol. PP, no. 99, pp. 1–11, early access 2015.

[12] Y. Yang, K. Zhou, H. Wang, F. Blaabjerg, D. Wang, and B. Zhang, "Frequency adaptive selective harmonic control for grid-connected inverters," *IEEE Trans. Power Electron.*, vol. 30, no. 7, pp. 3912–3924, Jul. 2015.

[13] M.A. Herran, J.R. Fischer, S.A. Gonzalez, M.G. Judewicz, I. Carugati, and D.O. Carrica, "Repetitive control with adaptive sampling frequency for wind power generation systems," *IEEE J. Emerg. Sel. Top. Power Electron.*, vol. 2, no. 1, pp. 58–69, Mar. 2014.

[14] M. Rashed, C. Klumpner, and G. Asher, "Repetitive and resonant control for a single-phase grid-connected hybrid cascaded multilevel converter," *IEEE Trans. Power Electron.*, vol. 28, no. 5, pp. 2224–2234, May 2013.

[15] A. Garcia-Cerrada, O. Pinzon-Ardila, V. Feliu-Batlle, P. Roncero-Sanchez, and P. Garcia-Gonzalez, "Application of a repetitive controller for a three-phase active power filter," *IEEE Trans. Power Electron.*, vol. 22, no. 1, pp. 237–246, Jan. 2007.

[16] S.A. Khajehoddin, M. Karimi-Ghartemani, P.K. Jain, and A. Bakhshai, "A resonant controller with high structural robustness for fixed-point digital implementations," *IEEE Trans. Power Electron.*, vol. 27, no. 7, pp. 3352–3362, Jul. 2012.

[17] M. Liserre, R. Teodorescu, and F. Blaabjerg, "Multiple harmonics control for three-phase grid converter systems with the use of PI-RES current controller in a rotating frame," *IEEE Trans. Power Electron.*, vol. 21, no. 3, pp. 836–841, May 2006.

[18] A.G. Yepes, F.D. Freijedo, O. Lopez, and J. Doval-Gandoy, "High-performance digital resonant controllers implemented with two integrators," *IEEE Trans. Power Electron.*, vol. 26, no. 2, pp. 563–576, Feb. 2011.

[19] J. C. Boemer, K. Burges, P. Zolotarev, J. Lehner, P. Wajant, M. Fürst, R. Brohm, and T. Kumm, "Overview of German grid issues and retrofit of photovoltaic power plants in German for the prevention of frequency stability problems in abnormal system conditions of the ENTSO-E region continental Europe," in *Proc. of 1st Solar Int. Workshop*, vol. 24, Oct. 2011.

[20] T. Ackermann, A. Ellis, J. Fortmann, J. Matevosyan, E. Muljadi, R. Piwko, P. Pourbeik, E. Quitmann, P. Sorensen, H. Urdal, and B. Zavadil, "Code shift: Grid specifications and dynamic wind turbine models," *IEEE Power Energy Mag.*, vol. 11, no. 6, pp. 72–82, Nov. 2013.

[21] M. Tsili and S. Papathanassiou, "A review of grid code technical requirements for wind farms," *IET Renew. Power Gener.*, vol. 3, no. 3, pp. 308–332, Sept. 2009.

[22] Z. Cao and G.F. Ledwich, "Adaptive repetitive control to track variable periodic signals with fixed sampling rate," *IEEE/ASME Trans. Mechatron.*, vol. 7, no. 3, pp. 378–384, Sept. 2002.

[23] D.J. Hogan, F. Gonzalez-Espin, J.G. Hayes, G. Lightbody, and M.G. Egan, "Adaptive resonant current-control for active power filtering within a microgrid," in *Proc. of ECCE*, Sept. 2014, pp. 3468–3475.

[24] F.D. Freijedo, A.G. Yepes, J. Malvar, O. Lopez, P. Fernandez-Comesana, A. Vidal, and J. Doval-Gandoy, "Frequency tracking of digital resonant filters for control of power converters connected to public distribution systems," *IET Power Electron.*, vol. 4, no. 4, pp. 454–462, 2011.

[25] M. Mascioli, M. Pahlevani, and P. Jain, "Frequency-adaptive current controller for grid-connected renewable energy systems," in *Proc. of INTELEC*, Sept. 2014, pp. 1–6.

[26] S. Gomez Jorge, C.A. Busada, and J.A. Solsona, "Frequency-adaptive current controller for three-phase grid-connected converters," *IEEE Trans. Ind. Electron.*, vol. 60, no. 10, pp. 4169–4177, Oct. 2013.

[27] F. González-Espín, G. Garcerá, I. Patrao, and E. Figueres, "An adaptive control system for three-phase photovoltaic inverters working in a polluted and variable frequency electric grid," *IEEE Trans. Power Electron.*, vol. 27, no. 10, pp. 4248–4261, Oct. 2012.

[28] Y. Yang, K. Zhou, and F. Blaabjerg, "Frequency adaptability of harmonics controllers for grid-interfaced converters," *Int'l J. Control*, pp. 1–12, DOI: 10.1080/00207179.2015.1022957, 2015.

[29] K. Nishida, T. Ahmed, and M. Nakaoka, "Cost-effective deadbeat current control for wind-energy inverter application with LCL filter," *IEEE Trans. Ind. Appl.*, vol. 50, no. 2, pp. 1185–1197, Mar./Apr. 2014.

[30] K. Zhou, Y. Yang, F. Blaabjerg, and D. Wang, "Optimal selective harmonic control for power harmonics mitigation," *IEEE Trans. Ind. Electron.*, vol. 62, no. 2, pp. 1220–1230, Feb. 2015.

[31] R. Costa-Castello, J. Nebot, and R. Grino, "Demonstration of the internal model principle by digital repetitive control of an educational laboratory plant," *IEEE Trans. Education*, vol. 48, no. 1, pp. 73–80, Feb. 2005.

[32] T.I. Laakso, V. Valimaki, M. Karjalainen, and U.K. Laine, "Splitting the unit delay - FIR/all pass filters design," *IEEE Signal Processing Mag.*, vol. 13, no. 1, pp. 30–60, Jan. 1996.